THE JOURNAL OF PHYSICAL CHEMISTRY LETTERS
A JOURNAL OF THE AMERICAN CHEMICAL SOCIETY

pubs.acs.org/JPCL

Letter

The Dynamical Ensemble of the Posner Molecule Is Not Symmetric

Shivang Agarwal, Clarice D. Aiello, Daniel R. Kattnig, and Amartya S. Banerjee*

Cite This: *J. Phys. Chem. Lett.* 2021, 12, 10372–10379

Read Online

ACCESS | Metrics & More | Article Recommendations | Supporting Information

ABSTRACT: The Posner molecule, $Ca_9(PO_4)_6$, has long been recognized to have biochemical relevance in various physiological processes. It has found recent attention for its possible role as a biological quantum information processor, whereby the molecule purportedly maintains long-lived nuclear spin coherences among its ^{31}P nuclei (presumed to be symmetrically arranged), allowing it to function as a room temperature qubit. The structure of the molecule has been of much dispute in the literature, although the S_6 point group symmetry has often been assumed and exploited in calculations. Using a variety of simulation techniques (including *ab initio* molecular dynamics and structural relaxation), rigorous data analysis tools, and by exploring thousands of individual configurations, we establish that the molecule predominantly assumes low-symmetry structures (C_s and C_i) at room temperature, as opposed to the higher-symmetry configurations explored previously. Our findings have important implications for the viability of this molecule as a qubit.

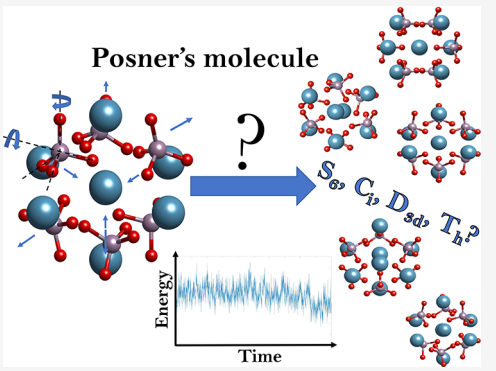

The calcium phosphate trimer, $Ca_9(PO_4)_6$, is of special biological interest. First discovered in the bone mineral hydroxyapatite in 1975 by Betts and Posner,[1] and henceforth coined the Posner molecule (PM), it is thought to form the structural building block of amorphous calcium phosphate.[2] Its presence in simulated body fluids was confirmed by Onuma and Ito,[3] and its aggregation has been hypothesized to underpin bone growth.[4−7] More recently, it has been proposed that the ^{31}P nuclear spins within PMs can maintain long-lived entanglement and that this could play an important role in nervous excitation via synaptic Ca^{2+} ion release.[8−10] These and other studies[11] have subsequently explored PMs as potential "neural qubits", drawing upon the fact that nuclear spin coherence times associated with these systems have been found to be exceptionally large per theoretical estimates. Such studies have suggested or assumed that the prototypical structure for the PM is one with an S_6 molecular point group symmetry, at least on average.[10] Furthermore, in the presence of a well-defined rotation axis of the cluster (such as the 3-fold C_3 rotational symmetry of the supposed S_6 symmetric cluster), the binding and unbinding of PMs could arguably act as a "pseudospin" entangler of the nuclear spin states of multiple PMs, which is a necessary precondition for the "quantum brain" concept, as suggested in ref 10.

In the context of the aforementioned mechanism, molecular point group symmetries for PMs are important because they dictate the form of the spin−spin coupling network. The number of independent components in this network is directly related to the point group symmetry of the structure.[12] Certain molecular symmetries can render the six ^{31}P nuclei magnetically equivalent (e.g., S_6), resulting in a small number of unique scalar (J) couplings (e.g., three unique coupling constants for S_6).[11] Understandably, other molecular symmetries could treat groups of ^{31}P nuclei as distinct, thus resulting in a larger number of pertinent scalar couplings.[13] As the ability of the system to sustain long-lived spin coherences is starkly related to the asymmetry in the coupling network,[14−18] the spin physics of PMs is inherently linked to the molecule's point group symmetries. Further, the presence of an inversion center in the PM, as found for S_6, would render the intracluster dipolar coupling block-diagonal in a basis of well-defined parity under exchange of two ^{31}P nuclei related by inversion. As a consequence, the inclusion of a singlet-polarized diphosphate molecule in such a cluster could generate long-lived spin population differences, spared from fast spin relaxation by the dipolar coupling within the PM.

The structure of the isolated PM is unknown. However, a series of studies[2,10,11,19] suggest a high degree of symmetry, e.g., S_6 and beyond, which was later exploited[10] in deriving the molecule's hypothetical entanglement-driven interaction mechanisms.[11,20] That the symmetry of the cluster might in fact be lower, has, on the other hand, been pointed out as early as 2003 in the work of Yin et al.[4] and then later in refs 20 and 11. On the basis of studies of the PM so far, two possibilities ought to be addressed: (a) could the molecule exist as a stable entity, i.e.,

Received: August 25, 2021
Accepted: October 13, 2021

https://doi.org/10.1021/acs.jpclett.1c02796
J. Phys. Chem. Lett. 2021, 12, 10372−10379

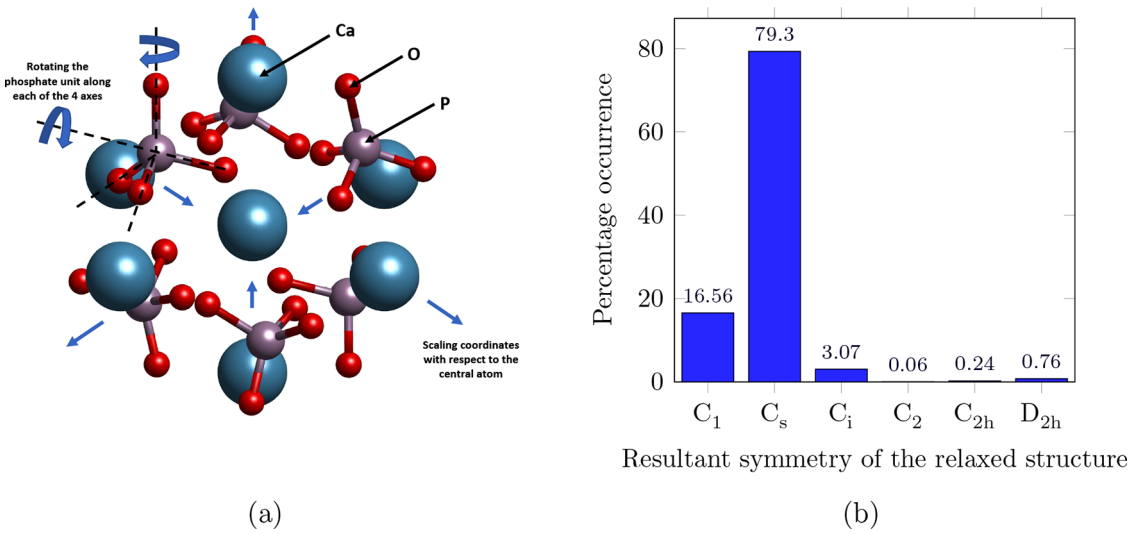

Figure 1. (a) The scheme used for creating over 10 000 structures by rotating the phosphate units and scaling all the coordinates with respect to the central atom. The blue, purple, and red spheres represent Ca, P, and O atoms, respectively. (b) Percentage occurrence of each point group symmetry after *ab initio* structural relaxation of over 10 000 initial structures (DFT with B3LYP hybrid functional and 6-311G(d,p) basis set).

corresponding to a minimum on the potential energy surface (PES), of high symmetry that is dominantly populated at physiological temperatures, as motivated by refs 2 and 19, or (b) could thermal fluctuations average the molecule's geometry to an effective structure of high symmetry, i.e., of an overall S_6 symmetry, despite the ensemble comprising predominantly low-symmetry states, as advocated in ref 10? Reference 10 reports the energy difference between S_6 and C_1 to be 0.06 eV = 1.53 meV/atom = 2.33 k_BT, while ref 19 suggests an alternate value of 0.13 eV = 3.33 meV/atom = 5.06 k_BT between S_6 and C_2, suggesting that these structures are thermally accessible, thereby highlighting the importance of probing hypothesis (b) by studying the dynamical ensemble properties. Indeed, Swift et al.,[10] while utilizing the S_6-symmetry in deriving the specifics of the quantum brain hypothesis, acknowledge the existence of multiple, more stable structures of lower symmetries. Moreover, it was understood that they considered nonequilibrated structures, assumed to exist in the average, for their calculations.[21] Naturally, considering a more symmetric yet less stable molecular structure has important implications on its spin properties, and prior works[2,19,22] could have suffered from the use of poor basis sets available at the time and the use of molecular force fields rather than *ab initio* methods. Molecular dynamics-based studies[23] using improved force fields[24,25] suggest the less symmetric point group C_3 for the molecule as well. Thus, given the conflicting state of the literature on the one the hand, and the importance of the existence of highly symmetric Posner clusters in support of recent quantum biological hypotheses on the other hand, we were prompted to conclusively re-examine the structure of the PM.

Since the PM is a calcium phosphate trimer, we performed initial simulations on the monomer $Ca_3(PO_4)_2$ and dimer $Ca_6(PO_4)_4$ configurations to validate our simulation setup. As detailed in the Supporting Information, the symmetry of the optimized monomer structure agreed with previous studies.[19,22] For the dimer, the work of Kanzaki et al.[22] was followed closely, and many of their structures were replicated. These results gave us confidence to pursue the structural symmetry of the PM, which is discussed below.

As the PM is hypothesized to exist in a variety of molecular symmetries,[10,19,22] we set out to identify symmetric minima on the PES of the molecule. To cover an appreciable portion of the PES of the PM, we used various techniques to set up the initial atomic positions and different analysis techniques to extract the relevant data, as detailed below.

First, a wide variety of possible structures were created by modifying some of the techniques used in previous studies.[22] This resulted in over 10 000 viable structures. A schematic representation of the method can be seen in Figure 1a, and further details are provided in the Supporting Information. In all cases, once the molecular structure was optimized using *ab initio* structural relaxation, the resultant configuration had low symmetry, i.e., either C_s, C_i, or no symmetry (C_1). Figure 1b shows the distribution of the observed symmetries of the relaxed structures obtained by the described strategy. It is evident that the PES of the PM is dominated by low-symmetry structures.

Second, the atoms were arranged in relatively high-symmetry configurations "by hand" without giving any consideration to the existence and initial stability of the structure or to the forces on the individual atoms. The rationale was that since none of the previous structures resulted in one of the high-symmetry structures reported in earlier studies, the molecule might instead transition into one of these high-symmetry structures if the starting configuration was constrained in symmetry. Structures with symmetries such as S_6, T_h, C_{3v}, and D_{3d} were constructed. The molecular structures were perturbed slightly from their original symmetries and optimized. However, for all of the four above-mentioned symmetries, when subjected to structural relaxation, the molecule failed to retain or increase the point-group symmetry and, instead, tumbled down to a low-symmetry structure—C_i or C_s—as was also the case in our previous approach. Structural relaxation with solvent effects included via a polarizable continuum model (PCM)[26,27] did not result in high-symmetry structures either. Finally, to verify that our results were not an artifact of the particular basis set, exchange correlation functional, or simulation software in use, we repeated our calculations using a semilocal exchange correlation functional and a plane-wave DFT code and obtained very similar results.

https://doi.org/10.1021/acs.jpclett.1c02796
J. Phys. Chem. Lett. 2021, 12, 10372−10379

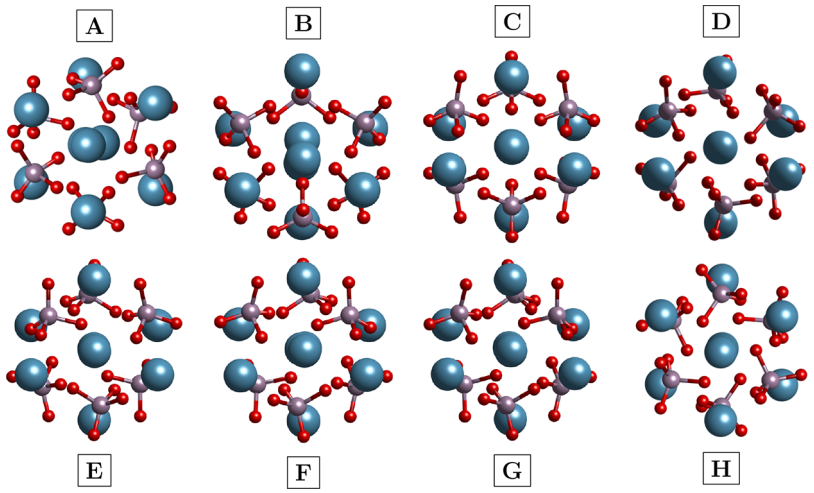

Figure 2. Eight different structures that were used as starting geometries for dynamical simulations of the PM. The labels (A–H) used in the manuscript are stated.

Table 1. Point Group Symmetries for Each of the Structures in Figure 2, Their Formation Energies, As Well As the Point Group Symmetries Displayed by Each Configuration during a Dynamical Simulation/Evolution over 22.8 ps[a]

transition structure index	symmetry prior to the creation of the transition structure	transition structure point group symmetry	formation energy (in eV) of the transition structure	resultant symmetries over dynamical runs
A	C_s	C_s	−271.660	C_1, C_2, C_s, D_{2h}
B	C_{3v}	C_{3v}	−269.555	C_1, C_2, C_s, C_{2h}, C_{3v}, D_{2h}
C	D_{3d}	D_{3d}	−264.997	C_1, C_s, C_i, T, C_{2h}, D_{2h}, D_{3d}
D	D_{3d}	C_{2h}	−269.551	C_1, C_s, C_i, T, C_{2v}, C_{2h}, D_{2h}
E	S_6	C_i	−271.552	C_1, C_s, C_i, C_2, T, C_{2h}, D_{2h}
F	S_6	C_i	−271.540	C_1, C_s, C_i, T, C_{2h}, D_{2h}
G	S_6	D_{2h}	−271.239	C_1, C_s, C_i, T, C_{2h}, D_{2h}, O_h
H	T_h	D_{2h}	−269.531	C_1, C_s, C_i, C_2, C_{2v}, C_{2h}, D_{2h}

[a]In comparison, the formation energy for a monomer calcium phosphate was calculated to be −84.244 eV. The listed formation energies of all trimer configurations are lower than three times this value.

Next, noting that the S_6 symmetry has been so widely discussed and accepted, an S_6 symmetric structure was built using an alternative technique. The phosphate units were considered as rigid tetrahedrals. The force field developed by Demichelis et al.[25] was used to model the atomic interactions. Imposing the S_6 symmetry enables the parametrization of the structure in terms of 10 parameters. Following a symmetry-constrained global minimization of the system's energy based on the above parameters, a unique structure was obtained, details of which can be found in the Supporting Information. Using DFT with the B3LYP hybrid functional and a 6-311G(d,p) basis, it was identified as a transition state structure and subjected to further geometrical relaxation. The optimized structure exhibited a C_i symmetry—starkly lower in symmetry than the initial S_6 symmetry. When performed under constrained symmetry, the same *ab initio* geometrical relaxation calculation failed to reach self-consistency. Thus, the optimization of symmetric structures modeled on existing force fields also failed to produce stable structures with low symmetries.

As our exhaustive search using structural relaxation failed to identify symmetric species, we then studied the dynamical properties of eight semistable Posner structures by *ab initio* molecular dynamics (AIMD). Starting structures were obtained from the supposedly minimum energy structures in ref 19, resymmetrized and subjected to *ab initio* structural optimization (using DFT with the B3LYP hybrid functional and the BP86/Def2TZVPP/W06 basis set). At the end of the relaxation procedure, they had low forces on the atoms (on the order of 10^{-4} eV/Å). However, these structures did not correspond to energy minima but were transition states of higher order instead. Distorting these structures along the normal modes associated with imaginary frequencies followed by further optimization of these structures resulted in the molecule tumbling to lower symmetries, as did the formation of these structures without the symmetry constraints. We considered the eight unique molecular structures derived through the above procedure. These, along with the corresponding molecular point group symmetries, as obtained by the Visual Molecular Dynamics (VMD) software[28] are displayed in Figure 2. We also performed vibrational spectrum calculations on these transition state structures and compared them with an existing spectrum,[10] details of which can be found in the Supporting Information. The structures were then studied by AIMD using the same basis set and DFT functional as above, at two different temperatures, 298 K (room temperature) and 315 K (at the higher end of human metabolic temperatures), to see if they maintain their high symmetry or give rise to high-symmetry species in the time average. The molecules were allowed to evolve for a total time of about 24 ps, in which the first 1.2 ps—or the first 5% of the total time—were considered to be the equilibration phase of the molecule and were not considered for subsequent analyses. Further details related to this particular choice of total simulation time is available in the Supporting Information.

https://doi.org/10.1021/acs.jpclett.1c02796
J. Phys. Chem. Lett. 2021, 12, 10372−10379

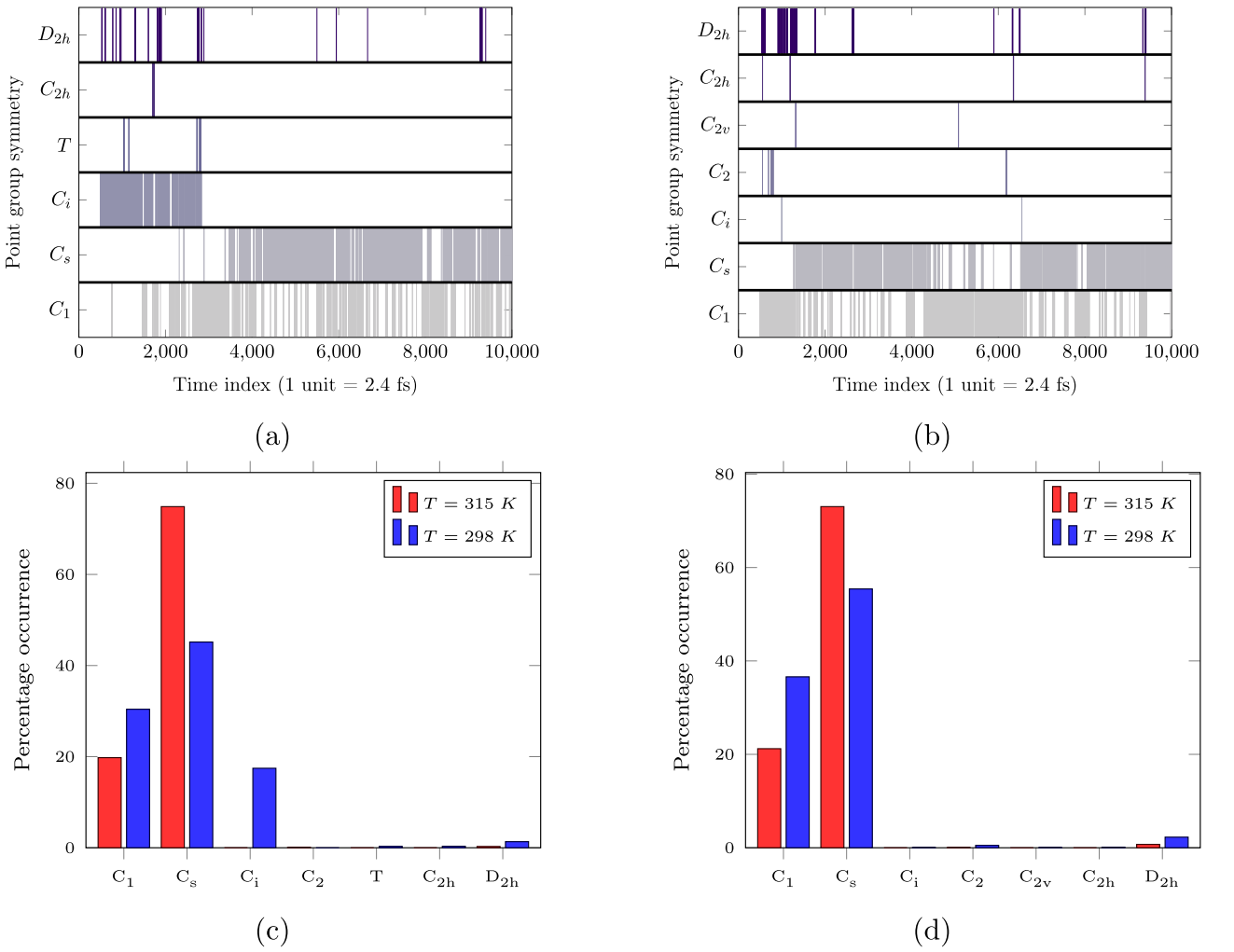

Figure 3. Time persistence of symmetries and the associated frequency of occurrence of each symmetry for two different starting configurations over a dynamical run. In the figure, (a) and (c) represent the data for configuration C, whereas (b) and (d) represent data for configuration H. Note that (a) and (b) represent the data at T = 298 K, and thus some additional symmetries which were observed at T = 315 K are not present in these plots.

At the end of each of the eight dynamical runs, and at both of the above-mentioned temperatures, the PM exhibited either a C_s or a C_i point group symmetry. Thus, it was understood that, even if the molecule is forced to exist in a relatively higher symmetry state, as imposed by our method, it will naturally tumble down to one of the lower-symmetry states within picoseconds. This leads us to argue that any stable configuration of the PM is likely to exhibit lower symmetries at room temperature.

Time averages and temporal variations in the molecule's symmetry were then studied as it appeared plausible that the molecule might exhibit a symmetric structure in the temporal average. Specifically, we studied the point group symmetries and energies of the $\mathcal{N} = 9500$ structures generated during each AIMD run. This allowed us to infer time persistence of the molecule's symmetry, if present. We observed that the molecule does indeed exhibit a variety of symmetries within the time frame considered, as visualized in Figure 3a,b. However, the higher symmetries were observed only fleetingly, i.e., on time scales of the order of 100 fs—too short to be significant, both as an independent species or to markedly determine the average structure. This supports our claim that the PM prefers to exist in low molecular symmetries. Moreover, as exemplified by Figure 3, we can say that the behavior described above of low-symmetry configurations throughout the dynamical evolution is consistent among all the eight unique structures in Figure 2. Further details can be found in the Supporting Information.

Even if the PM exhibits higher symmetries only fleetingly, it may *appear* as a more symmetric structure in the time average. To test this possibility, time-averaged structures for entire dynamical runs were created and studied. To this end, the translational and rotational motion of the molecule was eliminated via a rigid-body realignment procedure, and the aligned $\mathcal{N}$ structures were averaged. A single-point calculation was realized for these time-averaged structures, and their energies were compared. In addition to averaging all the $\mathcal{N}$ structures, an average structure was also obtained for subsets of potentially higher symmetry structures in the dynamical runs, which we define as the most symmetric molecular point group observed in a single dynamical run—e.g., D_{2h} for the cases of Figure 3a,b. Specifically, the subset of structures chosen for averaging from the entire range of these high-symmetry phases of structures was the longest consecutively occurring group of structures. For instance, in Figure 3b, this would correspond to the group of D_{2h} structures located just after the 1000th time index. Note that we refrained from obtaining an average structure for all of the high-symmetry structures because different high-symmetry structures might have emerged throughout the AIMD runs. Figure 4 provides a representation

https://doi.org/10.1021/acs.jpclett.1c02796
J. Phys. Chem. Lett. 2021, 12, 10372−10379

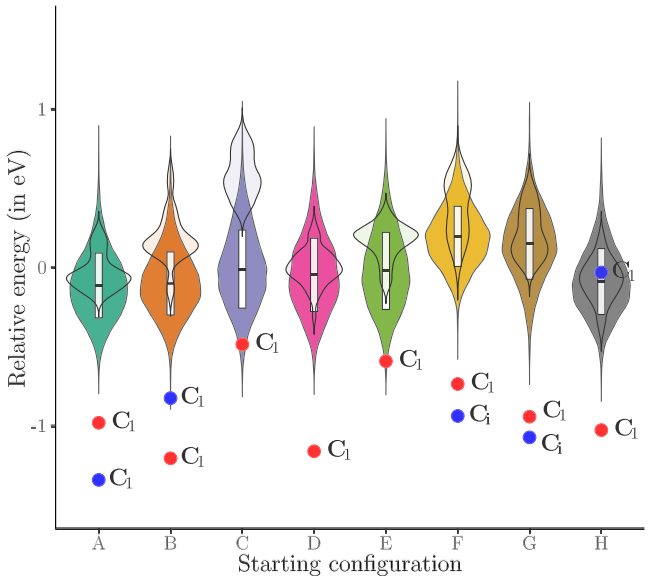

Figure 4. Energy spread of the dynamical runs for each of the starting configurations listed in Figure 2 represented by kernel density estimations in the form of vertical violin plots. The blue dots represent the energy of the time-average structure over the entire dynamical run, and the red dot represents the energy of the time-average structure of that subset of the high-symmetry phase that is present for the longest continuous duration. The point-group symmetry of the averages is indicated next to the symbols. The semitransparent overlays on each of the violin plots represent the energy distribution for the entire high-symmetry phase. The most stable high-symmetry phases for each of the cases were D_{2h}, D_{2h}, C_{2h}, D_{2h}, C_{2h}, D_{2h}, D_{2h}, and D_{2h}, respectively. Dots missing from the graph were found at energies higher than the scale of the figure. The plot also shows the mean and standard deviation of the energy spread within the representations of probability density functions in the form of white boxes. The energies reported are within the numerical accuracy of the method and basis set used.[30,31]

of the energy distributions over the AIMD runs together with a comparison of single-point energies and point group symmetries of the time-averaged structures. It can be seen that the energy spread between all averaged structures is relatively small—about 1.36 eV on average. Whenever the N intermediate structures were averaged, regardless of the initial configuration of the molecule, the point group symmetry of the averaged structure was either C_1, C_i, or C_s, which, for the purposes of this study, have been considered as "low symmetries". Their energies are shown as blue dots. This further reinforces the hypothesis that the PM prefers to exist in lower point group symmetries at any time as well as on average, at biologically relevant temperatures. Additionally, when looking at the energies of only the temporary high-symmetry phases of the PM which, in Figure 4, have been represented by the semitransparent violin plots overlaid on top of the opaque plots which represent the energies of the entire dynamical run, one can see that the energy of the structures with a higher symmetry is higher than the average energy, which agrees with our claim. However, seemingly in contrast to the above observation, we observe that the time-average structure of the higher symmetry phase can have a lower energy than the time-average structure of the entire dynamical run. This, however, can be explained by the fact that in every studied case, the time-averaging of even a high-symmetry phase yielded a structure with low (C_i or C_s) symmetry. Thus, the lower energy individual structures always possess low symmetries, and the data do not invalidate the claim that lower symmetries are preferred. We also mention in passing that we have carried out our point group symmetry analysis using more than one software package (VMD and WebMO[29]) and obtained similar results. Further details can be found in the Supporting Information.

On the basis of the above analyses, we identified the most stable structure of the PM to be the overall time-average structure of the configuration A, which can be seen as a blue dot in Figure 4. Notably, the point group symmetry for this structure is C_1, i.e., no symmetry. At the same time, we reiterate that the PMs possibly exist in an ensemble of structures and that identifying a singular structure as the dominant PM structure is incorrect. More information about configuration A and its atomic coordinates can be found in the Supporting Information.

With our calculations unable to convincingly point us toward a PM structure with high symmetry, we performed principal component analysis (PCA) on the data from the dynamical runs. It was expected that, if the molecule exhibits any kind of high symmetry that might have been overlooked in our symmetry analysis methodology, the associated high-symmetry structure would show up as one of the dominant eigenmodes of the PCA. However, none of the dominant eigenmodes displayed any kind of high symmetry. In fact, in all cases, the eigenmodes had either a C_i or a C_s point group symmetry. Moreover, as can be seen in Figure 5a,c,e, each configuration yielded one predominant eigenmode. Similar plots and figures for all dynamical runs can be found in the Supporting Information. While the maximum displacement of an atom in this mode from its corresponding position in the time-average structure over the entire dynamical run was small—less than 0.3 Å—this mode, instead, reflected a more appreciable displacement of the phosphates due to their rotation. Structures corresponding to the first three dominant modes did not give way to higher symmetries. The small observed fluctuations further emphasize that considering an average structure over our dynamical data set was appropriate. A detailed PCA for all other considered structures is provided in the Supporting Information.

We next resorted to another powerful data analysis technique, namely, *k*-means clustering, to identify hidden patterns in the data generated from our dynamical runs that might not have been revealed by our earlier attempts. It was found that, for each of the eight starting configurations, the ideal number of clusters describing our data sets was 2 and that the associated mean structure for each cluster had low point group symmetry—C_1 or C_i. This further agrees with the data and analyses that have already been presented above and with our assessment that the PM mostly exists as an ensemble of low-symmetry structures. Clustering results for all eight configurations are provided in the Supporting Information.

In summary, we have explored the dynamical structural properties of the PM. Our results do not indicate a predominant S_6 molecular symmetry. Instead, we argue that the molecule exists within a spread of multiple lower-symmetry structures at room temperature. We also explored the most stable form of the PM in a vacuum (concordant with earlier work) as well as in the presence of water (using a PCM), evaluated the point group symmetry in these scenarios, and came to conclusions corroborating our dynamical calculations. We used a variety of simulation techniques, including structural relaxation and molecular dynamics calculations, both at the level of empirical force fields, and using density functional theory based on semilocal and hybrid exchange correlation functionals as well as dispersion corrected functionals.[32] These calculations have been done assuming the isolated PM in a vacuum or a dielectric

https://doi.org/10.1021/acs.jpclett.1c02796
J. Phys. Chem. Lett. 2021, 12, 10372−10379

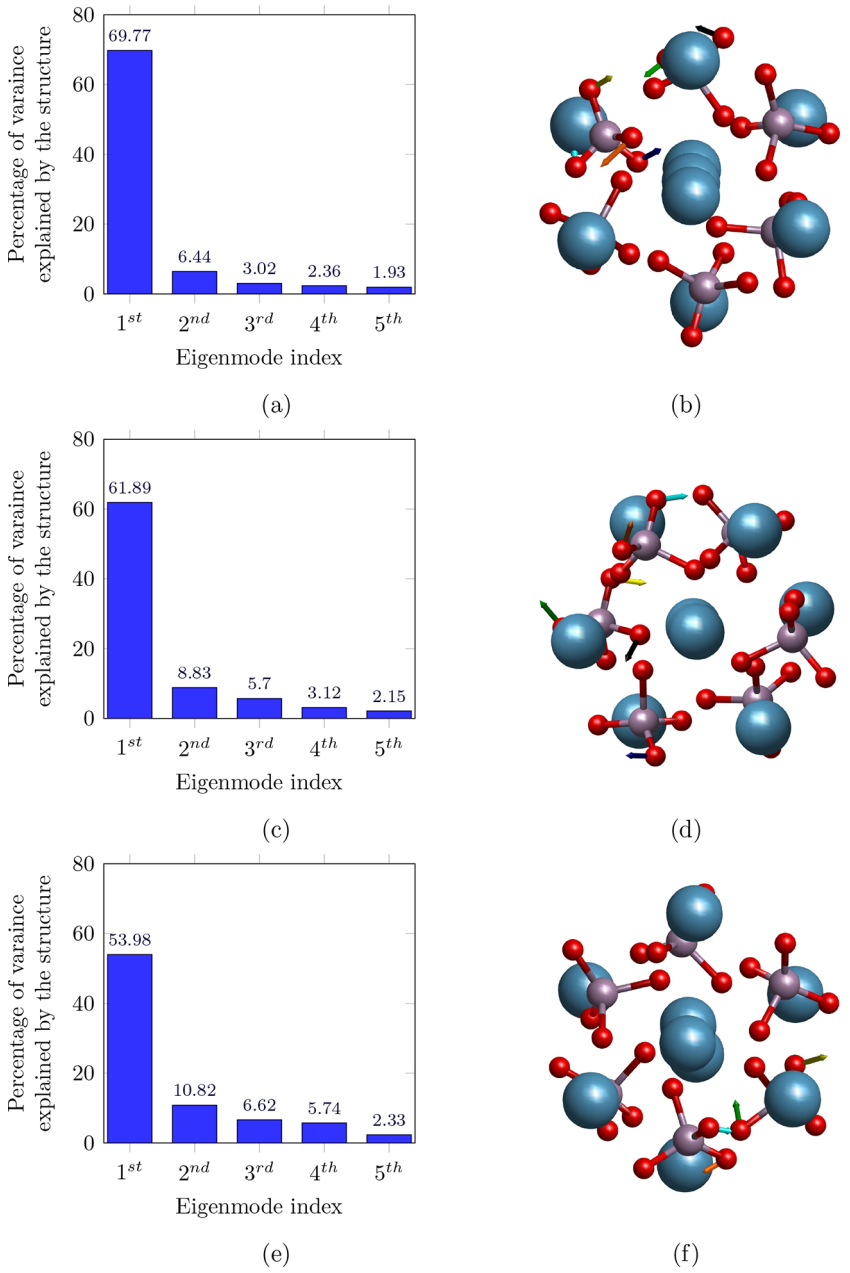

Figure 5. (a, c, e) Eigenvalues resulting from PCA over a single dynamical run for configurations E, D, and B respectively. One predominant mode is observed. (b, d, f) Difference between the most dominant eigenmode and the time-average structure of the corresponding dynamical run. The arrows have been elongated three-fold for clarity.

continuum. Similar calculations in the presence of a non-homogenous intracellular fluid around the PM are expected to hinder the molecule's rotation and likely further reduce the cluster's point group symmetry, which will lead to faster relaxation of the ^{31}P coherences.[11] To interpret the results of our simulations, we employed a variety of structural analysis tools, including vibrational spectra calculations and the evaluation of time persistence of symmetries, as well as a broad spectrum of data analysis tools, including structural averaging, PCA, and *k*-means clustering. The exploration of thousands of individual molecular configurations, the focus on dynamical structural properties at room temperature, and the use of a wide variety of simulation and data analysis tools are all distinguishing features of our work, and together they serve to provide robustness to our conclusions.

Our extensive analysis of the dynamical and structural properties of the Posner molecule suggests that it predominantly exists in low-symmetry molecular structures such as C_s, C_i, and C_1 at room temperature, as opposed to the results of previous studies suggesting a prototypical S_6 symmetric structure. Moreover, the initial configuration of the molecule often dictates the geometric configurations through which the molecule transitions during a dynamical run. Most of these transition structures exhibit low molecular point group symmetries; the high-symmetry phases are found to be present only fleetingly and have thus been assumed to be unimportant. Average structures were also found to be of low symmetry. Our results indicate that that the molecule does not naturally exhibit a 3-fold axis of rotation, such as present in S_6, in a vacuum or in a homogeneous solvent. Calculation of spin−spin coupling

https://doi.org/10.1021/acs.jpclett.1c02796
J. Phys. Chem. Lett. 2021, 12, 10372−10379

constants and spin coherence times for the structures explored by us constitutes ongoing and future work.

Lastly, we suggest the possibility of experimental verifications of our results. At a very basic level, it may well be possible to establish the existence of Posner molecules in simulated body fluids by introducing the constituents at stoichiometric ratios. Imaging techniques such as Dynamic Light Scattering or Transmission Electron Microscopy and NMR spectroscopy could then be applied to observe/study the basic properties of these molecules.[8] However, we believe that more sophisticated techniques, possibly following established quantum optics protocols and using microfluidics, might be needed to confirm or refute the possibility of the Posner molecule sustaining ^{31}P qubit states.

COMPUTATIONAL METHODS

For structural relaxation, we used Quantum ESPRESSO[33] with the Standard Solid-State Pseudopotentials library[34,35] and the Perdew−Burke−Ernzerhof (PBE) exchange correlation functional and Q-Chem[36] with both PBE and B3LYP exchange-correlation functionals, and a basis set of 6-311G(d,p) for the atomic orbitals. Symmetries were analyzed using two toolkits, VMD and WebMO.[29] Both toolkits gave the same symmetries. Further details about our methods can be found in the Supporting Information.

ASSOCIATED CONTENT

Supporting Information

The Supporting Information is available free of charge at https://pubs.acs.org/doi/10.1021/acs.jpclett.1c02796.

Ab initio molecular dynamics, geometry optimization, solvation files (ZIP)

Details about our methods, results of our simulations on monomers and dimers, data obtained from dynamical runs, vibrational analysis, PCA, and *k*-means, along with our identified most stable structure of the Posner molecule (PDF)

AUTHOR INFORMATION

Corresponding Author

Amartya S. Banerjee − *Department of Materials Science and Engineering, University of California, Los Angeles 90095, United States;* orcid.org/0000-0001-5916-9167; Email: asbanerjee@ucla.edu

Authors

Shivang Agarwal − *Department of Electrical and Computer Engineering, University of California, Los Angeles 90095, United States*

Clarice D. Aiello − *Department of Electrical and Computer Engineering, University of California, Los Angeles 90095, United States*

Daniel R. Kattnig − *Department of Physics and Living Systems Institute, University of Exeter, Exeter EX4 4QD, U.K.;* orcid.org/0000-0003-4236-2627

Complete contact information is available at: https://pubs.acs.org/10.1021/acs.jpclett.1c02796

Notes

The authors declare no competing financial interest.

ACKNOWLEDGMENTS

The authors would like to thank Michael W. Swift for insightful discussions, which helped with the preparation of the manuscript. The authors would also like to thank UCLA's Institute for Digital Research and Education (IDRE) for making available the computing resources used in this work. D.R.K. would like to thank the Office of Naval Research for financial support (ONR Award Number N62909-21-1-2018).

REFERENCES

(1) Posner, A. S.; Betts, F. Synthetic amorphous calcium phosphate and its relation to bone mineral structure. *Acc. Chem. Res.* **1975**, *8*, 273−281.

(2) Treboux, G.; Layrolle, P.; Kanzaki, N.; Onuma, K.; Ito, A. Symmetry of Posner's cluster. *J. Am. Chem. Soc.* **2000**, *122*, 8323−8324.

(3) Onuma, K.; Ito, A. Cluster growth model for hydroxyapatite. *Chem. Mater.* **1998**, *10*, 3346−3351.

(4) Yin, X.; Stott, M. J. Biological calcium phosphates and Posner's cluster. *J. Chem. Phys.* **2003**, *118*, 3717−3723.

(5) Du, L.-W.; Bian, S.; Gou, B.-D.; Jiang, Y.; Huang, J.; Gao, Y.-X.; Zhao, Y.-D.; Wen, W.; Zhang, T.-L.; Wang, K. Structure of clusters and formation of amorphous calcium phosphate and hydroxyapatite: from the perspective of coordination chemistry. *Cryst. Growth Des.* **2013**, *13*, 3103−3109.

(6) Dey, A.; Bomans, P. H. H.; Muller, F. A.; Will, J.; Frederik, P. M.; de With, G.; Sommerdijk, N. A. J. M. The role of prenucleation clusters in surface-induced calcium phosphate crystallization. *Nat. Mater.* **2010**, *9*, 1010−1014.

(7) Wang, L.; Li, S.; Ruiz-Agudo, E.; Putnis, C. V.; Putnis, A. Posner's cluster revisited: direct imaging of nucleation and growth of nanoscale calcium phosphate clusters at the calcite-water interface. *CrystEngComm* **2012**, *14*, 6252−6256.

(8) Fisher, M. P. Quantum cognition: The possibility of processing with nuclear spins in the brain. *Ann. Phys.* **2015**, *362*, 593−602.

(9) Weingarten, C. P.; Doraiswamy, P. M.; Fisher, M. A new spin on neural processing: quantum cognition. *Front. Hum. Neurosci.* **2016**, *10*, 541.

(10) Swift, M. W.; Van de Walle, C. G.; Fisher, M. P. A. Posner molecules: from atomic structure to nuclear spins. *Phys. Chem. Chem. Phys.* **2018**, *20*, 12373−12380.

(11) Player, T. C.; Hore, P. Posner qubits: spin dynamics of entangled $Ca_9(PO_4)_6$ molecules and their role in neural processing. *J. R. Soc., Interface* **2018**, *15*, 20180494.

(12) Buckingham, A.; Love, I. Theory of the anisotropy of nuclear spin coupling. *J. Magn. Reson.* **1970**, *2*, 338−351.

(13) Perras, F. A.; Bryce, D. L. Symmetry-amplified J splittings for quadrupolar spin pairs: a solid-state NMR probe of homoatomic covalent bonds. *J. Am. Chem. Soc.* **2013**, *135*, 12596−12599.

(14) Annabestani, R.; Cory, D. G. Dipolar relaxation mechanism of long-lived states of methyl groups. *Quantum Inf. Process.* **2018**, *17*, 1−25.

(15) Lidar, D. A. *Quantum Information and Computation for Chemistry*; John Wiley & Sons, Ltd, 2014; pp 295−354, DOI: 10.1002/9781118742631.ch11.

(16) Feng, Y.; Theis, T.; Wu, T.-L.; Claytor, K.; Warren, W. S. Long-lived polarization protected by symmetry. *J. Chem. Phys.* **2014**, *141*, 134307.

(17) Vinogradov, E.; Grant, A. K. Long-lived states in solution NMR: Selection rules for intramolecular dipolar relaxation in low magnetic fields. *J. Magn. Reson.* **2007**, *188*, 176−182.

(18) Stevanato, G.; Roy, S. S.; Hill-Cousins, J.; Kuprov, I.; Brown, L. J.; Brown, R. C.; Pileio, G.; Levitt, M. H. Long-lived nuclear spin states far from magnetic equivalence. *Phys. Chem. Chem. Phys.* **2015**, *17*, 5913−5922.

(19) Treboux, G.; Layrolle, P.; Kanzaki, N.; Onuma, K.; Ito, A. Existence of Posner's cluster in vacuum. *J. Phys. Chem. A* **2000**, *104*, 5111−5114.

(20) Lin, T.-J.; Chiu, C.-C. Structures and infrared spectra of calcium phosphate clusters by ab initio methods with implicit solvation models. *Phys. Chem. Chem. Phys.* **2018**, *20*, 345−356.
(21) Swift, M. Private communication, 2020.
(22) Kanzaki, N.; Treboux, G.; Onuma, K.; Tsutsumi, S.; Ito, A. Calcium phosphate clusters. *Biomaterials* **2001**, *22*, 2921−2929.
(23) Mancardi, G.; Tamargo, C. E. H.; Di Tommaso, D.; De Leeuw, N. H. Detection of Posner's clusters during calcium phosphate nucleation: a molecular dynamics study. *J. Mater. Chem. B* **2017**, *5*, 7274−7284.
(24) Ainsworth, R. I.; Tommaso, D. D.; Christie, J. K.; de Leeuw, N. H. Polarizable force field development and molecular dynamics study of phosphate-based glasses. *J. Chem. Phys.* **2012**, *137*, 234502.
(25) Demichelis, R.; Garcia, N. A.; Raiteri, P.; Innocenti Malini, R.; Freeman, C. L.; Harding, J. H.; Gale, J. D. Simulation of calcium phosphate species in aqueous solution: force field derivation. *J. Phys. Chem. B* **2018**, *122*, 1471−1483.
(26) Truong, T. N.; Stefanovich, E. V. A new method for incorporating solvent effect into the classical, ab initio molecular orbital and density functional theory frameworks for arbitrary shape cavity. *Chem. Phys. Lett.* **1995**, *240*, 253−260.
(27) Barone, V.; Cossi, M. Quantum calculation of molecular energies and energy gradients in solution by a conductor solvent model. *J. Phys. Chem. A* **1998**, *102*, 1995−2001.
(28) Humphrey, W.; Dalke, A.; Schulten, K. VMD − Visual Molecular Dynamics. *J. Mol. Graphics* **1996**, *14*, 33−38.
(29) Polik, W. F.; Schmidt, J. WebMO: Web-based computational chemistry calculations in education and research. *Wiley Interdiscip. Rev. Comput. Mol. Sci.* e1554, DOI: 10.1002/wcms.1554.
(30) Weigend, F.; Ahlrichs, R. Balanced basis sets of split valence, triple zeta valence and quadruple zeta valence quality for H to Rn: Design and assessment of accuracy. *Phys. Chem. Chem. Phys.* **2005**, *7*, 3297−3305.
(31) Weigend, F. Accurate Coulomb-fitting basis sets for H to Rn. *Phys. Chem. Chem. Phys.* **2006**, *8*, 1057−1065.
(32) Grimme, S.; Antony, J.; Ehrlich, S.; Krieg, H. A consistent and accurate ab initio parametrization of density functional dispersion correction (DFT-D) for the 94 elements H-Pu. *J. Chem. Phys.* **2010**, *132*, 154104.
(33) Giannozzi, P.; Baroni, S.; Bonini, N.; Calandra, M.; Car, R.; Cavazzoni, C.; Ceresoli, D.; Chiarotti, G. L.; Cococcioni, M.; Dabo, I.; et al. QUANTUM ESPRESSO: a modular and open-source software project for quantum simulations of materials. *J. Phys.: Condens. Matter* **2009**, *21*, 395502.
(34) Prandini, G.; Marrazzo, A.; Castelli, I. E.; Mounet, N.; Marzari, N. Precision and efficiency in solid-state pseudopotential calculations. *NPJ. Comput. Mater.* **2018**, *4*, 1−13.
(35) Lejaeghere, K.; Bihlmayer, G.; Björkman, T.; Blaha, P.; Blügel, S.; Blum, V.; Caliste, D.; Castelli, I. E.; Clark, S. J.; Dal Corso, A.; et al. Reproducibility in density functional theory calculations of solids. *Science* **2016**, *351*, 351.
(36) Shao, Y.; Gan, Z.; Epifanovsky, E.; Gilbert, A. T.; Wormit, M.; Kussmann, J.; Lange, A. W.; Behn, A.; Deng, J.; Feng, X.; et al. Advances in molecular quantum chemistry contained in the Q-Chem 4 program package. *Mol. Phys.* **2015**, *113*, 184−215.

https://doi.org/10.1021/acs.jpclett.1c02796
J. Phys. Chem. Lett. 2021, 12, 10372−10379